


Cultivation and characteristics of partial nitrification granular sludge in a sequencing batch reactor inoculated with heterotrophic granules

Jianfang Wang^{1,2,3} · Feiyue Qian^{1,2}  · Xiaopeng Liu¹ · Wenru Liu⁴ · Shuyong Wang¹ · Yaoliang Shen^{1,2}

Received: 3 April 2016 / Revised: 12 June 2016 / Accepted: 9 August 2016 / Published online: 24 August 2016
© Springer-Verlag Berlin Heidelberg 2016

Abstract The aim of this study was to develop a simple operation strategy for the cultivation of partial nitrification granules (PNGs) treating an autotrophic medium. For this strategy, aerobic granular sludge adapted to high concentration organics removal was seeded in a sequencing batch reactor (SBR) with a height/diameter ratio of 3.8, and the ratio of organics to the ammonia nitrogen-loading rate (C/N ratio) in the influent was employed as the main control parameter to start up the partial nitrification process. After 86 days of operation, the nitrite accumulation rate reached 1.44 kg/(m³ day) in the SBR, and the removal efficiency of ammonia nitrogen (NH₄⁺-N) was over 95 %. The PNGs showed a dense and compact structure, with an excellent settling ability, a typical extracellular polymeric substance (EPS) composition, and a high ammonia oxidation activity. The high-throughput pyrosequencing results indicated that the microbial

community structure in the granules was significantly influenced by the C/N ratio, and ammonia-oxidizing bacteria (AOB), including the r-strategist *Nitrosomonas* and k-strategist *Nitrospira* genre, which accounted for approximately 40 % of the total biomass at the end of operation. The effective suppression of nitrite-oxidizing bacteria (NOB) growth was attributed to oxygen competition on the granular surface among functional bacteria, as well as the high free ammonia or free nitrous acid concentrations during the aeration period.

Keywords Aerobic granular sludge · Partial nitrification · Influent characteristics · Selective inhibition · High-throughput pyrosequencing

Electronic supplementary material The online version of this article (doi:10.1007/s00253-016-7797-9) contains supplementary material, which is available to authorized users.

✉ Feiyue Qian
feiyuehandler@163.com

¹ College of Environmental Science and Engineering, Suzhou University of Science and Technology, No. 1 Kerui Road, 215009 Suzhou, People's Republic of China

² Jiangsu Collaborative Innovation Center of Technology and Material of Water Treatment, No. 1 Kerui Road, 215009 Suzhou, People's Republic of China

³ College of Tianping, Suzhou University of Science and Technology, No. 55 Changjiang Road, 215009 Suzhou, People's Republic of China

⁴ College of Environmental Science and Engineering, Tongji University, No. 1239 Siping Road, 200092 Shanghai, People's Republic of China

Introduction

The biological nitrogen removal process using anaerobic ammonium oxidation (anammox) has been successfully applied in hundreds of wastewater treatment plants worldwide and has been shown to be an efficient and economical technical system (Lackner et al. 2014). However, the stable supply of nitrite for anammox bacteria for use as an electron acceptor remains a major obstacle for applying this new technology in full-scale systems, because it is difficult to achieve the partial oxidation of influent ammonia nitrogen (NH₄⁺-N) to nitrite (NO₂⁻-N) by ammonia-oxidizing bacteria (AOB), while full nitrification to nitrate (NO₃⁻-N) by nitrite-oxidizing bacteria (NOB) is avoided during the operation of conventional bioreactors (Ma et al. 2016). Compared to activated sludge systems, aerobic granular sludge represents excellent settling properties, which allow a larger amount of slow-growing AOB biomass retained in the reactors, and makes it possible to treat higher ammonia loaded wastewater. (Vázquez-Padín et al. 2010).

Moreover, the special spatial structure of granules, creating a significant mass transfer gradient, would benefit to suppress NOB distributed in the interior layer (Perez et al. 2014). According to previous reports, the typical nitrite accumulation rate (NAR) in a SHARON reactor with flocculent sludge is always less than $0.1 \text{ kg}/(\text{m}^3 \text{ day})$, whereas much higher values of $0.5\text{--}6.0 \text{ kg}/(\text{m}^3 \text{ day})$ in granular ones could be accomplished (Mosquera-Corral et al. 2005; Bartroli et al. 2010; Jemaat et al. 2014; Wei et al. 2014). In other words, the reactor volume required to treat a certain ammonia loading would be much smaller by working with granules.

However, the cultivation of partial nitrification granules (PNGs) treating an autotrophic medium is relatively difficult in full-scale engineering systems, since both sludge granulation and partial nitrification need to be achieved and maintained simultaneously. The evidences provided by Kishida et al. (2012) and Cydzik-Kwiatkowska and Wojnowska-Baryła (2011) suggested that mature nitrifying granules could be successfully harvested after 40–80 days of operation, by inoculating heterotrophic granular sludge into a continuous stirred tank (CSTR) and sequencing batch reactor (SBR) with a typical geometry, and it was much shorter than the start-up period of 120–160 days with flocculent sludge being seeded (Shi et al. 2010; Chen et al. 2015). Therefore, a similar approach would be taken into account to cultivate PNGs, while high ammonia loading rate, sufficient hydraulic selection pressure, and appropriate dissolved oxygen (DO), pH, and temperature conditions were applied to achieve high efficient nitrite accumulation, by enriching AOB and inhibiting NOB in the granules (Park et al. 2010; Ganigué et al. 2012; Show et al. 2012).

To assess the feasibility of shifting from high-concentration organics removal to partial nitrification in a SBR with a low column height/diameter (h/d) ratio and inoculated with excess heterotrophic granular sludge, the ratio of organics to the ammonia nitrogen-loading rate (C/N ratio) in the influent was used as the main operational parameter in the present study. During two successive phases, changes in sludge morphology and functional bacteria activities were also evaluated using scanning electron microscopy (SEM) and the specific oxygen uptake rate (SOUR), respectively. In addition, the evolution of microbial characteristics in the granules was analyzed using a high-throughput pyrosequencing technique to identify the primary factor responsible for accumulating high nitrite levels.

Materials and methods

Reactor setup and operation

The experiment was carried out in a lab-scale SBR with a working volume of 4.0 L and h/d of 3.8. Fine air bubbles were supplied through a gas diffuser at the bottom of the reactor,

with an airflow rate of 2.5 L/min. Throughout the experiment, the DO concentration was maintained at $2.5\text{--}7 \text{ mg}/\text{L}$. The SBR was operated on a 3-h cycle, which included 5 min of influent filling, 166/169 min of aeration, 6/3 min of settling, and 3 min of effluent discharging from the middle port of the reactor with a volumetric exchange ratio of 40 %. A time controller was installed to allow the sequential operation of the SBR. The temperature was maintained at $25 \pm 1 \text{ }^\circ\text{C}$ using a water bath.

Seed sludge and wastewater composition

Seed aerobic granular sludge adapted to the removal of organic carbon (as sodium acetate) was obtained from another SBR with a h/d of 10 that had been operated at an organics loading rate (OLR) of $4.5 \text{ kg}/(\text{m}^3 \text{ day})$ and C/N ratio of 10, with a chemical oxygen demand (COD) removal efficiency of approximately 90 %. The seed sludge was milky and had a compact and round-shaped structure (Fig. S1), mean size of 1.5 mm, and sludge volume index after 5 min of sedimentation (SVI₅) of 26 mL/g. The ratio of mixed liquor volatile suspended solids (MLVSS) to mixed liquor suspended solids (MLSS) was approximately 0.45, and the initial MLSS concentration in the reactor was 7700 mg/L.

Synthetic wastewater with the following composition was used in this study: 0–1400 mg/L COD (as sodium acetate), 200–500 mg/L $\text{NH}_4^+\text{-N}$ (as ammonium chloride), 112 mg/L K_2HPO_4 , 20 mg/L $\text{MgSO}_4 \cdot 7\text{H}_2\text{O}$, 4 mg/L $\text{FeSO}_4 \cdot 2\text{H}_2\text{O}$, 40 mg/L $\text{CaCl}_2 \cdot 2\text{H}_2\text{O}$, and 1.0 mL of trace solution per liter (Liu et al. 2008). The pH value was adjusted to 7.8–8.2 by adding NaHCO_3 , with the molar ratios of bicarbonate to $\text{NH}_4^+\text{-N}$ at 1.1–1.2:1. Table 1 shows the exact water quality indicators of the influent during the different operation periods. In phase I, the influent COD concentration gradually decreased, while the influent $\text{NH}_4^+\text{-N}$ was fixed at 200 mg/L, resulting in a decrease in the C/N ratio from 4.5/0.6 to 0.6/0.6. To promote the development of the nitrifying bacteria community, inorganic wastewater was employed in the following phase, and the influent $\text{NH}_4^+\text{-N}$ concentration was progressively increased from 200 to 500 mg/L.

Analytical methods

MLSS, MLVSS, SVI₅, COD, $\text{NH}_4^+\text{-N}$, $\text{NO}_2^-\text{-N}$, and $\text{NO}_3^-\text{-N}$ were measured using the procedure described in Standard Methods (APHA 1998). The pH value and DO concentration were monitored with PB-10 (Sartorius, Germany) and H1946N portable meters (WTW, Germany), respectively. The size distribution of the granules was measured regularly using different sieves with opening sizes of 0.80, 1.25, 1.60, 2.00, and 2.50 mm, and the arithmetic mean value of granular diameter was equal to the sum of products of dry weight percentages and the average size in intervals.

Table 1 Detailed influent water quality indicators of the SBR during different operation periods

Phase	Time (days)	Influent concentration (mg/L)		Volumetric loading rate (kg/(m ³ day))		C/N ratio
		COD	NH ₄ ⁺ -N	COD	NH ₄ ⁺ -N	
I	1~8	1400 ± 20	200 ± 6	4.5	0.6	4.5/0.6
	9~16	1300 ± 19	200 ± 6	4.0	0.6	4.0/0.6
	17~21	1000 ± 30	200 ± 6	3.3	0.6	3.3/0.6
	22~26	800 ± 10	200 ± 6	2.6	0.6	2.6/0.6
	27~31	600 ± 12	200 ± 6	2.0	0.6	2.0/0.6
	32~40	400 ± 20	200 ± 6	1.3	0.6	1.3/0.6
	41~48	200 ± 11	200 ± 6	0.6	0.6	0.6/0.6
II	49~57	0	300 ± 8	0.0	0.9	0.0/0.9
	58~72	0	400 ± 5	0.0	1.3	0.0/1.3
	73~86	0	500 ± 2	0.0	1.6	0.0/1.6

The morphological shape of granular sludge was observed using a Quanta™ 250 scanning electron microscope (FEI, USA). To prepare the samples for SEM evaluation, the pre-treatment steps described by Wu et al. (2010) were followed, including fixation, washing, dehydration, and seasoning, and the samples were then sputter-coated with aurum. The extracellular polymeric substances (EPSs) were extracted using the formaldehyde-NaOH method, and the protein (PN) and polysaccharide (PS) contents were quantified using the Lowry and phenol-sulfuric acid methods, respectively (Adav and Lee 2008).

To determine the SOUR of heterotrophic bacteria (HeB), AOB, and NOB, represented by SOUR-H, SOUR-A, and SOUR-N, respectively, batch tests were carried out according to Bassin et al. (2012a). Granules of 0.5 g MLVSS were sampled from the SBR at the end of the operational cycle and aerated for 1 h to remove the bulk substances. A standard BOD bottle (250 mL) containing nutrient media without COD and nitrogen was aerated to achieve 100 % air saturation at 25 °C. Then, both biomass and concentrated stock solutions of either COD or ammonium/nitrite were added to start the reaction at pH 7.5 and 25 ± 1 °C. The initial concentrations of COD, NH₄⁺-N, and NO₂⁻-N were around 300, 100, and 100 mg/L, respectively. SOUR values were obtained by linear regression of DO (for endpoints higher than 3 mg/L) versus time divided by the constant amount of MLVSS, and the portion donated by endogenous respiration was deducted from the result. All batch experiments were performed in triplicate.

Calculations

The NAR of the reactor was calculated using the influent NH₄⁺-N loading rate (NLR) and nitrite accumulation percentage (NAP) in the effluent according to the following equation.

$$NAR \left(\frac{\text{kg}}{\text{m}^3 \text{ day}} \right) = NLR \times \frac{\text{NO}_2^- \text{-N}_{\text{eff}}}{\text{NO}_2^- \text{-N}_{\text{eff}} + \text{NO}_3^- \text{-N}_{\text{eff}}} \quad (1)$$

The free ammonia (FA) and free nitrous acid (FNA) concentrations were calculated as follows (Ford and Kachtick 1980), respectively.

$$FA \left(\frac{\text{mg}}{\text{L}} \right) = \frac{17}{14} \times \frac{\text{NH}_4^+ \text{-N} \times 10^{\text{pH}}}{\exp \left[\frac{6334}{(273+T)} \right] + 10^{\text{pH}}} \quad (2)$$

$$FNA \left(\frac{\text{mg}}{\text{L}} \right) = \frac{46}{14} \times \frac{\text{NO}_2^- \text{-N}}{\exp \left[\frac{-2300}{(273+T)} \right] \times 10^{\text{pH}}} \quad (3)$$

DNA extraction, PCR, and pyrosequencing

To analyze the microbial community structure, genomic DNA was extracted from sludge samples using the E.Z.N.A.® Soil DNA Isolation Kit (Omega Bio-tek, Inc., Norcross, USA) according to the manufacturer's protocol. The bacterial primers 338F (5'-ACTCCTACGGGAGGCAGC A-3') and 806R (5'-GGACTACHVGGGTWTCTAA T-3') were used to amplify the V3 and V4 regions of the 16S ribosomal RNA (rRNA) gene (Dennis et al. 2013). Polymerase chain reaction (PCR) was performed using a GeneAmp® 9700 thermal cycler (Applied Biosystems, USA), and the reaction mixture (20 µL) contained 4 µL of 5× FastPfu Buffer, 2 µL of dNTPs (0.5 mM), 0.8 µL of each primer (5 µM), 0.4 µL of FastPfu polymerase, and 10 ng of template DNA. The PCR conditions were 95 °C for 3 min, 27 cycles of denaturation at 95 °C for 30 s, annealing at 55 °C for 30 s, and extension at 72 °C for 45 s, followed by a final extension at 72 °C for 10 min. The PCR products were purified using the AxyPrep™ DNA Gel Extraction Kit (Axygen Biosciences, Union City, USA) according to the manufacturer's instructions and quantified using the QuantiFluor™-ST system (Promega, USA).

Following PCR, high-throughput pyrosequencing was conducted using the MiSeq technology (Illumina, USA) at Majorbio Bio-Pharm Technology Co., Ltd., Shanghai,

China. Operational taxonomic units (OTUs) were clustered with 97 % similarity cutoff values using UPARSE (version 7.1 <http://drive5.com/uparse/>), and chimeric sequences were identified and removed using UCHIME. The taxonomy of each 16S rRNA gene sequence was analyzed using RDP Classifier (<http://rdp.cme.msu.edu/>) against the SILVA 16S rRNA database using a confidence threshold of 70 % (Amato et al. 2013).

The raw sequence data had been deposited in the NCBI Sequence Read Archive database (accession number SRP073633).

Results

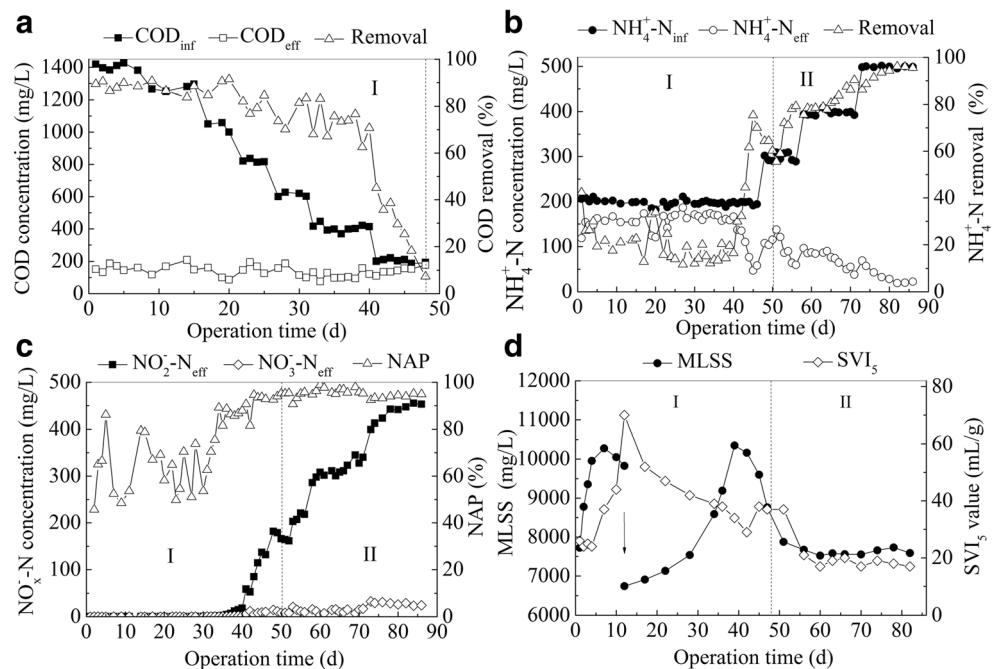
Reactor performance

The results for COD and NH_4^+ -N removal in SBR are shown in Fig. 1a, b, respectively. During phase I (days 1–48), the influent NH_4^+ -N concentration was kept constant at 200 mg/L, while the C/N ratio was gradually reduced from 4.5/0.6 to 0.6/0.6. The results showed that the COD removal efficiency decreased slowly from approximately 90 to 72 % in the first 40 days. In addition, the NH_4^+ -N removal of 19.5 ± 6.3 % was relatively low, with only 18.4 mg/L NO_2^- -N in the effluent on day 40 (Fig. 1c). Meanwhile, the portion of total N-species loss decreased from 24.4 ± 4.5 to 11.9 ± 4.2 % and shared the similar variation tendency as the influent COD concentration. A simultaneous nitrification-denitrification (SND) process occurring in the granules might not be neglected, since the assimilated nitrogen fraction was less than 5 % even at high

OLRs, based on the chemical formula for biomass of $\text{C}_5\text{H}_7\text{NO}_2$. An increase in MLSS from approximately 7700 mg/L on day 1 to over 10,000 mg/L on day 10 was observed, with a higher SVI_5 value, which was strongly associated with the rapid growth of HeB and a long settling time of 6 min in this phase (Fig. 1d). On day 12, the SVI_5 value exceeded the typical one of 50 mL/g for granular sludge (Cyzdik-Kwiatkowska and Wojnowska-Baryła 2011). To maintain the dominant position of the granules, the settling time for the SBR was reset to 3 min, with a stepwise decrease in the influent COD concentration. Despite the large biomass washout, the granular sludge had a high retention ability for microbes, and the MLSS concentration in the SBR increased again to 10,400 mg/L after another 30 days. In contrast to the first sludge growth period, SVI_5 improved significantly and was restored to the level of the seed sludge on day 40. When the influent C/N ratio reached 0.6/0.6, it was obvious that the partial nitrification performance of the reactor was enhanced significantly, as evidenced by the NH_4^+ -N removal and effluent NAP values increasing to the levels of 60 and 90 %, respectively, on day 48. And a balance between total N-species in the influent and effluent was almost accomplished. After a significant fluctuation in COD removal, it sharply decreased to below 10 % at the end of phase I, due to the heavy washout of HeB in granules caused by the limiting substrate (Fig. 1d).

Subsequently, in phase II (days 49–86), the progressive increase in NLR caused a further improvement in the NH_4^+ -N removal of the SBR, which increased from 60.2 % on day 50 to 95.9 % on day 84, as shown in Fig. 1b. In addition, a stable NAP of 90–97 % was achieved throughout

Fig. 1 COD (a) and NH_4^+ -N (b) removal and NO_2^- -N accumulation and NO_3^- -N performance of the SBR and variation of MLSS and SVI_5 (d) throughout the operation period



phase II. The NO_3^- -N concentration in the effluent was lower than 30 mg/L, even when the influent NH_4^+ -N concentration reached 500 mg/L. Moreover, it has been reported that the presence of slow-growing microbes, such as nitrifying bacteria, induces the formation of stable and compact granular sludge (Kishida et al. 2012; Chen et al. 2015). After 84 days of operation, a nitrite accumulating rate of 1.44 kg/(m³ day) for the reactor was achieved, and PNGs were successfully cultivated, while MLSS and SVI_5 were steadily maintained at 7600 mg/L and 17 mL/g, respectively. Although Wan et al. (2013) applied a high C/N ratio over 6:1 to start-up a partial nitrification process based on granular biomass in only 36 days, the operation period in this study was still much shorter than the typical one of 120~160 days using flocculent sludge to cultivate nitrifying granules treating high-strength NH_4^+ -N wastewater (Chen et al. 2015).

Sludge morphology

With the functional conversion of the reactor, apparent morphological changes in the aerobic granular sludge were also observed. Figure 2 shows the variation in the sludge particle size distributions in the SBR. During the start-up period, the growth of the seed granules in terms of particle size was effectively promoted by the high OLR. The highest mean diameter of the granular sludge was 2.0 mm on day 35 (C/N ratio of 1.3/0.6), as shown in Fig. S2a, while the fraction with a particle size >2.0 mm was more than 63.8 %. As the feed for the SBR was changed to the lower C/N ratio wastewater, the large granules (>2.0 mm) broke down into smaller ones, because of the HeB washout and the low cell yield of nitrifying

bacteria. The mature PNGs with brownish red (Fig. S2b) had a mean size of 1.4 mm at the end of operation, and the fraction with a particle size of 0.8~1.25 mm became the dominant one (35.2 %), with only 20.4 % of a particle size >2.0 mm. Vázquez-Padín et al. (2010) and Rathnayake et al. (2015) demonstrated that the penetration depth of oxygen in aerobic granular sludge varies typically in a range of 75~200 μm . The higher specific surface area of the small-sized granules was beneficial for the DO transport to the sludge surface, which could promote the growth of nitrifying bacteria at the outer edge.

Figure 3a–c clearly illustrates that at a relatively high OLR, the seed sludge was characterized by a round shape with dense and compact structure, which consisted of short rod, coccus, and filamentous bacteria that were cross-linked. After 84 days of operation, the PNGs had a spindle shape with an irregular profile, and their outer surface was covered with many straight rod bacteria, which might be adhered by a gel-like EPS matrix (Fig. 3d–f).

EPSs are believed to have a positive effect on the formation and stability of granular sludge or biofilm. Traditionally, PN is regarded to be the predominant component of the EPSs in aerobic granules with a high heterotrophic activity (Adav et al. 2008; Zhou et al. 2011). However, the content of PS, as a so-called bioglue, is greater than or equal to that of PN in the EPSs of nitrifying granules (Wu et al. 2012; Jemaat et al. 2014). Compared to HeB (such as *Pseudomonas*, *Zoogloea*, and *Flavobacteria*), the slow-growing nitrifying bacteria do not produce enough EPSs and barely achieve self-immobilization (Wu et al. 2012; Wan et al. 2014).

The EPS contents of the granular sludge throughout the entire operation were monitored by measuring PN and PS, and the results are shown in Table 2. The stepwise reduction in influent COD caused a significant decrease in the EPS content, which was accompanied by biomass detachment in the granular sludge. Meanwhile, the variation in the PN/PS ratio agrees with the general trend indicating that the granules had a high nitrifying activity. A similar phenomenon was also observed by Bassin et al. (2012b), when they enriched biofilms with nitrifying bacteria in moving bed biofilm reactors (MBBRs).

Kinetics study and microbe activities

To evaluate the responses of the functional bacteria to the operation conditions, kinetics studies at various C/N ratios were conducted in batch tests. The changes in the COD and N-species concentrations in a typical batch cycle on days 5, 48, and 84 are shown in Fig. 4, involving a time course of DO and pH values. The influent wastewater was fed into the SBR in 0~5 min, and the COD and NH_4^+ -N concentrations decreased significantly due to the dilution process.

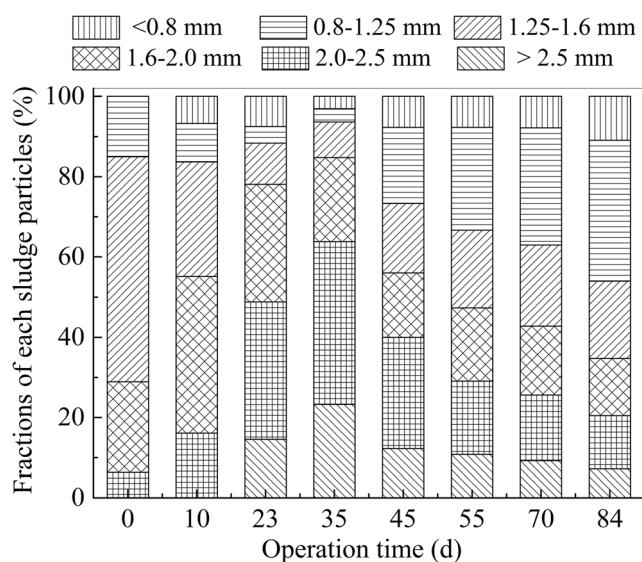


Fig. 2 Variation in the particle size distribution of sludge during the operation period

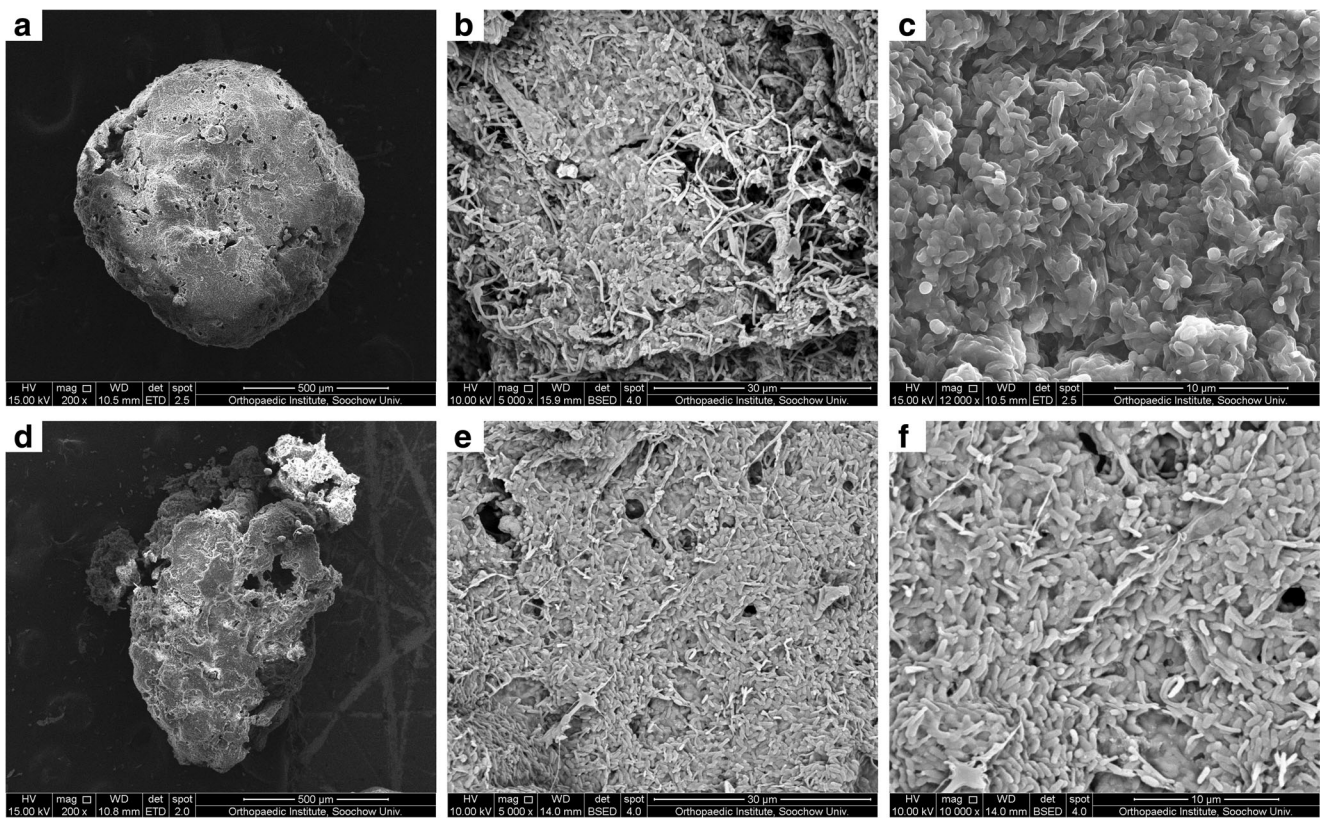


Fig. 3 SEM images of the seed sludge (a–c) and PNGs on day 84 (d–f)

On day 5, COD removal followed first-order kinetics ($R^2 = 0.9889$, $k = 0.051$ 1/min), while the maximum specific removal rate (q_{COD}) reached 161.0 mg/(g MLVSS h) during the first 30 min. In addition, the specific nitrification rate ($q_{\text{NH}_4\text{-N}}$), which was calculated as $\text{NH}_4^+\text{-N}$ removal, generally followed zero-order kinetics ($R^2 = 0.9881$) and had a very low value of 0.9 mg/(g MLVSS h). With the rapid degradation of acetate, both the DO and pH values sharply increased during the aeration, and a high FA concentration in the range 20.9–68.3 mg/L was also observed, as summarized in Table S1. At the end of phase I (day 48), the $q_{\text{NH}_4\text{-N}}$ of the granules reached 5.6 mg/(g MLVSS h), while q_{COD} decreased to 22.4 mg/(g MLVSS h) during the first 20 min. $\text{NO}_2^-\text{-N}$ accumulation also followed zero-order kinetics, and nitrate

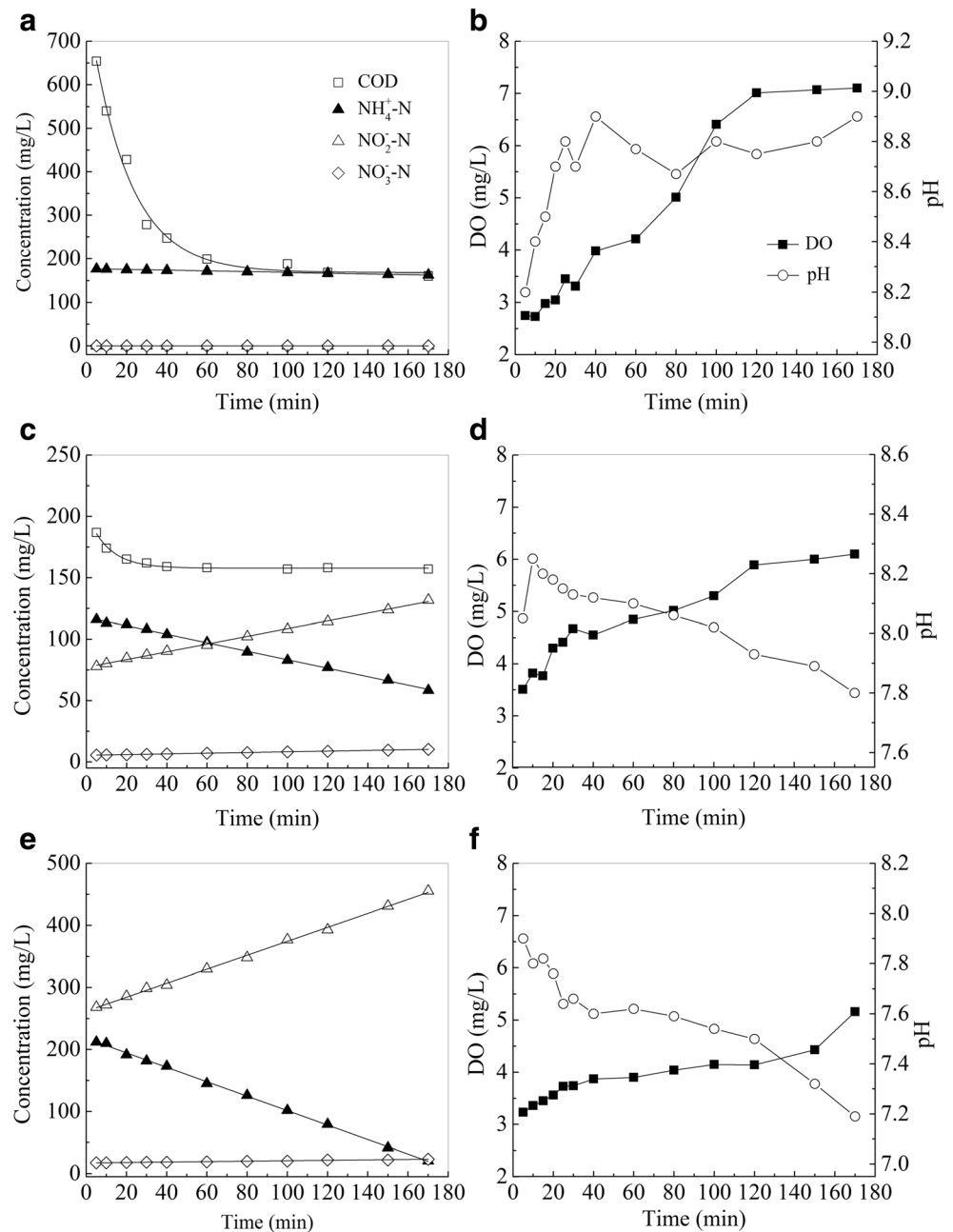
production was limited effectively. The changes in DO and pH were mainly controlled by nitrification, which caused the reduction in the FA concentration during the aeration. On day 84, the partial nitrification ability of the granules improved significantly, as $q_{\text{NH}_4\text{-N}}$ increased to 21.5 mg/(g MLVSS h), which was comparable with the values achieved in other nitrifying granular reactors in the range of 13.2–24.6 mg/(g MLVSS h) (Cyzdik-Kwiatkowska and Wojnowska-Baryła 2011; Isanta et al. 2015), but lower than the 33.6 mg/(g MLVSS h) reported by Bartroli et al. (2010). In addition, the specific $\text{NO}_2^-\text{-N}$ accumulation rate ($q_{\text{NO}_2\text{-N}}$) was 20.8 mg/(g MLVSS h), with a NAP of 95.1 %. Meanwhile, DO increased very slowly, and the FNA concentration (Table S1) at the end of aeration increased because of the accumulation of $\text{NO}_2^-\text{-N}$ and the decrease in pH.

In addition, SOUR values based on different substrate compositions were also used to indicate the HeB, AOB, and NOB activities (Fig. 5). As expected, the seed sludge was acclimated to organics removal and exhibited a low nitrification performance, and its SOUR-H was 6.4 and 36.2 times higher than its SOUR-A and SOUR-N, respectively. The operation strategy during phase I enhanced the AOB activity and suppressed both HeB and NOB, as SOUR-A was equal to 73.4 % of SOUR-H at the C/N ratio of 0.6/0.6. Afterward, AOB outcompeted the others because of the increasing influent $\text{NH}_4^+\text{-N}$ concentration, while SOUR-H decreased linearly to approximately 13.2 % of SOUR-A, and the highest SOUR-N

Table 2 EPS contents of granular sludge during different operation periods

Time (days)	C/N ratio	PN (mg/g)	PS (mg/g)	PN/PS ratio
1~7	4.5/0.6	125.1 ± 14.0	52.2 ± 16.7	2.40
22~26	2.6/0.6	80.5 ± 15.8	58.2 ± 4.6	1.38
32~40	1.3/0.6	54.9 ± 7.3	41.4 ± 8.9	1.33
42~47	0.6/0.6	55.6 ± 1.7	60.7 ± 3.8	0.99
50~58	0.0/0.9	52.5 ± 10.2	38.1 ± 7.2	1.38
58~72	0.0/1.3	40.7 ± 2.8	43.7 ± 4.4	0.93
74~82	0.0/1.6	41.6 ± 1.8	40.8 ± 1.1	1.02

Fig. 4 Changes in COD, NH_4^+ -N, NO_2^- -N, and NO_3^- -N concentrations and DO and pH values at different influent C/N ratios: **a, b** C/N = 4.5/0.6 (day 5), **c, d** C/N = 0.6/0.6 (day 48), and **e, f** C/N = 0/1.6 (day 84)



value was only 3.9 $\text{mg O}_2/(\text{g MLVSS h})$ at a C/N ratio of 0.0/1.6.

Microbial characteristics

Different sludge samples, including the seed sludge (S1) and granules sampled on day 48 (S2) and day 84 (S3), were subjected to high-throughput pyrosequencing to measure diversity of microbial community during the operation. A total of 36,069 qualified sequences and 399 OTUs were obtained for the community analysis at a similarity of 97 % (Table S2). The small number of OTUs was mainly attributed to the simple

composition of the synthetic wastewater. All sample coverage estimators were greater than 99.8 %, which indicated that the sequencing capacity could reflect the real microbial community compositions. In addition, both the richness and the diversity of the species were only slightly affected by the operation strategy. The Venn diagram in Fig. S3 shows that three sludge samples shared 95 OTUs, and the rarefaction curves for each sample are presented in Fig. S4.

The classifiable sequences of three sludge samples were affiliated with 19 phyla, 31 classes, and 112 genera. The predominant taxonomic group at the phylum level for the three sludge samples was *Proteobacteria* (a relative abundance of

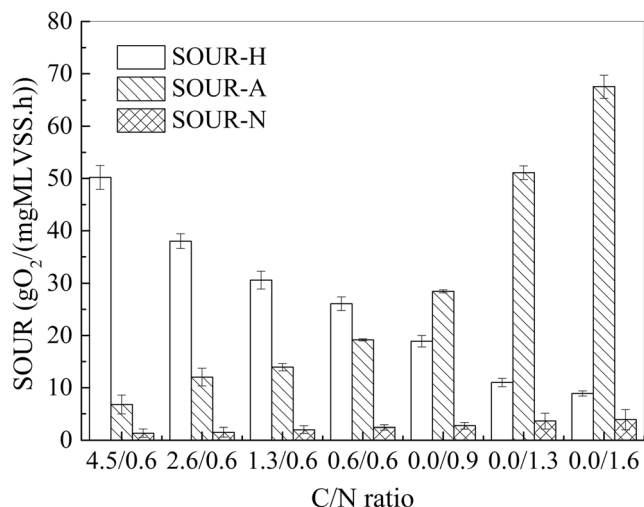


Fig. 5 The SOUR values of HeB, AOB, and NOB at different influent C/N ratios

68.6–82.3 %), followed by *Bacteroidetes* (9.5–28.4 %), which represented 91.5–97.5 % of all sequences, as shown in Table S3.

For the seed sludge, *Betaproteobacteria* (38.0 %), *Alphaproteobacteria* (34.0 %), *Deltaproteobacteria* (5.4 %), *Clostridia* (5.1 %), *Gammaproteobacteria* (4.0 %), *Flavobacteria* (2.7 %), and *Sphingobacteria* (2.3 %) were the most abundant groups at the class level, as shown in Fig. 6. These bacteria were widely distributed in the activated sludge (Wu et al. 2013) and granular biomass (Wan et al. 2014). As shown in Table 3 and Fig. S5, *Thauera* and *Paracoccus* were the most frequent genre in classes *Betaproteobacteria* and *Alphaproteobacteria*, respectively, and these HeB are usually present in organic matter oxidation and nitrifying-denitrifying activated sludge (Li et al. 2008, Liang et al. 2015). Meanwhile, nitrifying bacteria, including the genre *Nitrosomonas*, *Nitrospira*, and *Nitrospira*, only accounted for 0.05 % of the total bacteria in S1. Other

members, such as the genre *Flavobacterium* and *Pseudomonas*, are known to produce a glue-like EPS, which can adhere cells together.

Moreover, the HeB genera decreased significantly after 48 days operation in phase I, while the AOB fraction increased to become greater than the HeB fraction among the class of *Betaproteobacteria*. There were 1989 AOB sequences detected in S2, of which 99.7 % were related to the genus *Nitrospira*, and the remaining sequences were affiliated with the genus *Nitrosomonas* and the exact species *Nitrosomonas europaea*. Because the NOB growth was effectively suppressed, there were only 12 sequences related to the genus *Nitrospira*.

As described by Cydzik-Kwiatkowska and Wojnowska-Baryła (2011), AOB species diversity was improved by the stepwise increase in NLR (phase II), which was advantageous for the stability of the nitrification process. In S3, the genre *Nitrosomonas* (14.8 %) and *Nitrospira* (25.2 %) coexisted and dominated the total number of bacteria. Enrichment of AOB species with the NOB fraction below 0.15 % was consistent with variations in the functional bacteria activities in the granules as mentioned above. The relative abundance of AOB (approximately 40 %) in the nitrifying granules reached the average level reported in the literature (19.0–63.0 %), by using different molecular biology methods, such as FISH (Wu et al. 2012), real-time quantitative PCR (Matsumoto et al. 2010b; Cydzik-Kwiatkowska and Wojnowska-Baryła 2011), and high-throughput pyrosequencing (Rathnayake et al. 2015). The AOB fraction can be improved at higher NLR by increasing the number of *Nitrosomonas*-like species, which are believed to possess higher specific activities than *Nitrospira* species in ammonium-rich systems (Mobarry et al. 1997; Matsumoto et al. 2010a). Although the obvious washout of the genre *Thauera*, *Paracoccus*, *Hydrogenophaga*, *Flavobacterium*, and *Bdellovibrio* was demonstrated during the operation, the presence of HeB should not be

Fig. 6 The 20 dominant taxa found in each sample (S1 seed sludge, S2 sampled on day 48, S3 sampled on day 84) at the class level

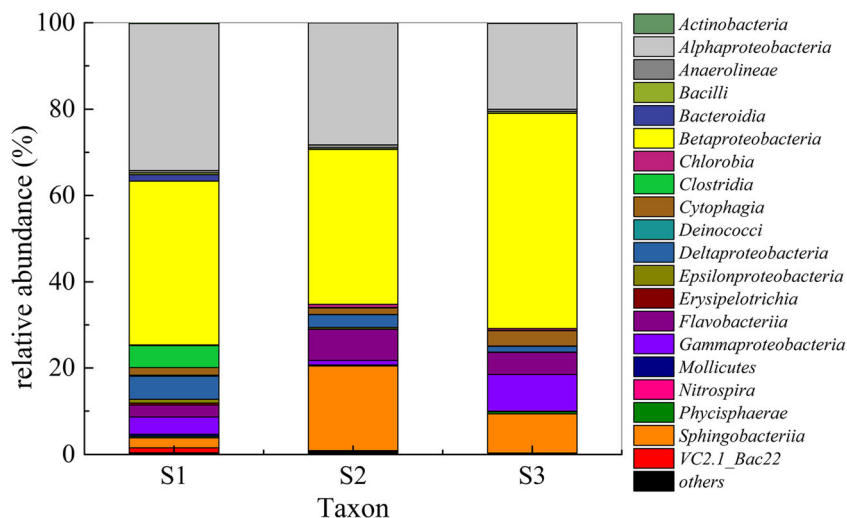


Table 3 Relative abundances of the main bacterial genre for each sample

Class	Genus	Percentage of sequences (%)		
		S1	S2	S3
<i>Betaproteobacteria</i>	<i>Nitrosomonas</i>	0.01	0.05	14.76
	<i>Nitrospira</i>	0.03	16.49	25.19
	<i>Thauera</i>	30.80	12.30	7.59
	<i>Hydrogenophaga</i>	5.78	1.26	0.72
	<i>Azoarcus</i>	0.67	4.08	0.47
<i>Alphaproteobacteria</i>	<i>Paracoccus</i>	23.97	8.22	2.43
	<i>Meganema</i>	2.79	15.50	9.71
	<i>Woodsholea</i>	3.43	1.85	2.36
<i>Deltaproteobacteria</i>	<i>Bdellovibrio</i>	4.07	2.45	0.86
<i>Clostridia</i>	<i>Fusibacter</i>	2.45	0.03	0.00
<i>Gammaproteobacteria</i>	<i>Arenimonas</i>	0.00	0.07	8.10
	<i>Pseudofulvimonas</i>	1.23	0.13	0.09
	<i>Pseudomonas</i>	1.80	0.21	0.05
<i>Flavobacteriia</i>	<i>Flavobacterium</i>	2.17	0.65	0.25
	<i>Fluviicola</i>	0.05	5.01	2.48
	<i>NS9_marine_group_norank</i>	0.17	0.34	1.02
<i>Sphingobacteriia</i>	<i>Saprospiraceae_uncultured</i>	0.67	19.25	8.50
<i>Nitrospira</i>	<i>Nitrospira</i>	0.01	0.10	0.13
<i>Cytophagia</i>	<i>Leadbetterella</i>	0.75	1.12	1.65
<i>Bacteroidia</i>	<i>vadinBC27</i>	1.14	0.00	0.00
Total		81.99	89.11	86.36

neglected. Matsumoto et al. (2010b) detected a significant amount of HeB, such as *Chloroflexi*, *Cytophaga-Flavobacterium-Bacteroides*, and *Proteobacteria*, in nitrifying granules, which was cultured with inorganic substrates after more than 1000 days. They concluded that HeB used the soluble microbial products released from nitrifying bacteria for growth because the sludge retention time was extremely long.

Discussion

As previously reported, the most important reason achieving a efficient and stable nitrite accumulation was the shift in the nitrifying microbial community in the granules. In this study, the high activity of AOB with the selective inhibition of NOB could be attributed to oxygen competition, in addition to their different tolerance capacities to the bulk FA and FNA concentrations.

It is generally accepted that heterotrophs have larger maximum specific growth rate coefficient (μ) and smaller oxygen half-saturation coefficient (K_O) values than autotrophs in activated sludge systems. At the beginning of phase I, although the DO concentration in the bulk liquid was always greater than 2.7 mg/L throughout the cycle, HeB, which predominated in the seed sludge, consumed massive amounts of oxygen

to oxidize the readily biodegradable organics, as a high COD removal being observed. The result was the limitation of the oxygen level on the granular surface, which may have been insufficient to meet the growth needs of nitrifying bacteria at high OLRs. Therefore, the decrease in the influent C/N ratio would enhance the AOB activity in the granules (Fig. 5). In addition, the accumulated NO_2^- -N concentration was always less than 1 mg/L over the first 30 days, the NOB growth was definitely suppressed owing to the substrate limitation. As the operation proceeded, the influent C/N ratio decreased to 0.6/0.6, resulting in the heavy washout of HeB and the growth promotion of AOB, especially the k-strategists with high affinities for ammonia and oxygen, such as *Nitrospira*. The result was evidenced by the high removal efficiency of NH_4^+ -N in the SBR and the high-throughput pyrosequencing results of S2. Meanwhile, the K_O values for NOB varied in the range 0.34–2.5 mg/L depending on the sludge size and oxygen diffusion conditions in the bioreactors, and these values were significantly higher than those for HeB (0.01–0.2 mg/L) and AOB (0.25–0.99 mg/L) (Van et al. 2010; Grady et al. 2011; Isanta et al. 2015). Thus, NOB would be vulnerable when competing for oxygen with the other groups. Moreover, a considerable amount of NH_4^+ -N at alkaline pH vales caused the FA concentration (Table S1) to exceed the typical inhibitory threshold for NOB ($K_{I,\text{NH}_3}^{\text{NOB}} = 0.1\text{--}4.0$ mg/L) but lower than the one for AOB ($K_{I,\text{NH}_3}^{\text{AOB}} = 10\text{--}150$ mg/L) (Sinha and

Annachhatre 2006; Ganigué et al. 2012), which could be the other reason for the extremely low fraction of NOB compared to AOB in S2. Importantly, a high FA level alone could not be used to wash out NOB in nitrifying granules without controlling other operational parameters. Chen et al. (2015) demonstrated complete nitrification with aerobic granular sludge at a NH_4^+ -N removal efficiency of 99 %, even when the maximum FA concentration reached 113 mg/L. It indicated that nitrifying bacteria embedded in granules would be more resistant to toxic substances than those in floc sludge.

When inorganic wastewater was fed into the SBR, the stepwise increase in the influent NH_4^+ -N concentration resulted in the enrichment of the r-strategist AOB *Nitrosomonas*, which have maximum specific NH_4^+ -N uptake rates of approximately 200 mg/(g MLVSS h) (Groeneweg et al. 1994). Although a large amount of excess nitrite was measured in the bulk liquid, an insufficient oxygen supply appeared to be the main factor that prevented the growth of the *Nitrobacter*-like, as a r-strategist NOB, which have low nitrite and oxygen affinities. There were only a few sequences related to genus *Nitrospira* in S3. During phase II, there was always some NH_4^+ -N left in the effluent of the SBR, and the extremely high SOUR-A replaced SOUR-H to create an oxygen-limiting environment. The results from the combined FISH-CLSM technique and DO microelectrode test clearly indicated that the obligate AOB usually occupied the active outer layer that was 70–200 μm thick and depleted most of dissolved oxygen in the aerobic granular sludge, whereas NOB existed close to them but were distributed in the interior layer (Chiu et al. 2007; Matsumoto et al. 2010b; Jemaat et al. 2014; Rathnayake et al. 2015). For these reasons, the spatial structure of the granules would benefit to suppress the NOB growth with the high oxygen diffusion resistance, while the same purpose was achieved in floc sludge systems by implementing an online aeration control strategy with an average DO of 0.1–0.25 mg/L (Ma et al. 2015). On the other hand, besides the high FA concentration at the initial aeration phase, the selective inhibition of accumulated FNA on *Nitrospira* cannot be neglected, because above 0.1 mg/L of FNA was between the inhibitory thresholds for NOB ($K_{I,\text{HNO}_2^{\text{NOB}}} = 0.01\sim 0.26$ mg/L) and AOB ($K_{I,\text{HNO}_2^{\text{AOB}}} = 0.49$ mg/L) (Zhou et al. 2011; Kim et al. 2012; Ganigué et al. 2012). Therefore, FA and FNA can be combined in an SBR to effectively suppress NOB in a single cycle by maintaining high concentrations of influent NH_4^+ -N and effluent NO_2^- -N.

In conclusion, the inoculation of heterotrophic granules is feasible for the start-up of a partial nitrification process in SBR, while the influent C/N ratio was chosen as a main control parameter to achieve both high ammonia removal efficiency and nitrite accumulation percentage. Microbial

community analysis clearly demonstrated that the enrichment of AOB species was accompanied by the obvious washout of HeB and the effective suppressing of NOB. It was in accord with variations in the functional bacteria activities in PNGs.

Acknowledgments This study was financially supported by National Natural Science Foundation of China (CN) (51308367, 51578353) and Natural Science Foundation of Jiangsu Higher Education (14KJB610009, 15KJB610013). We also acknowledge the support from the Preponderant Discipline Construction Project in higher education of Jiangsu Province, China. Jianfang Wang received the Jiangsu Government Scholarship for overseas studies.

Compliance with ethical standards

Ethical statement This article does not contain any studies with human participants or animals performed by any of the authors.

Conflict of interest The authors declare that they have no conflict of interest.

References

- Adav SS, Lee DJ (2008) Extraction of extracellular polymeric substances from aerobic granule with compact interior structure. *J Hazard Mater* 154:1120–1126
- Adav SS, Lee DJ, Tay JH (2008) Extracellular polymeric substances and structural stability of aerobic granule. *Water Res* 42:1644–1650
- Amato KR, Yeoman CJ, Kent A, Righini N, Carbonero F, Estrada A, Gaskins HR, Stumpf RM, Yildirim S, Torralba M, Gillis M, Wilson BA, Nelson KE, White BA, Leigh SR (2013) Habitat degradation impacts black howler monkey (*Alouatta pigra*) gastrointestinal microbiomes. *ISME J* 7:1344–1353
- APHA (1998) Standard methods for examination of water and wastewater, 20th ed. American Public Health Association, New York
- Bartoli A, Perez J, Carrera J (2010) Applying ratio control in a continuous granular reactor to achieve full nitrification under stable operating conditions. *Environ Sci Technol* 44:8930–8935
- Bassin JP, Kleerebezem R, Dezotti M, van Loosdrecht MCM (2012a) Measuring biomass specific ammonium, nitrite and phosphate uptake rates in aerobic granular sludge. *Chemosphere* 89:1161–1168
- Bassin JP, Kleerebezem R, Rosado AS, van Loosdrecht MCM, Dezotti M (2012b) Effect of different operational conditions on biofilm development, nitrification, and nitrifying microbial population in moving-bed biofilm reactors. *Environ Sci Technol* 46:1546–1555
- Chen FY, Liu YQ, Tay JH, Ning P (2015) Rapid formation of nitrifying granules treating high-strength ammonium wastewater in a sequencing batch reactor. *Appl Microbiol Biotechnol* 99:4445–4452
- Chiu ZC, Chen MY, Lee DJ, Wang CH, Lai JY (2007) Oxygen diffusion and consumption in active aerobic granules of heterogeneous structure. *Appl Microbiol Biotechnol* 75:685–691
- Cydzik-Kwiatkowska A, Wojnowska-Baryła I (2011) Nitrifying granules cultivation in a sequencing batch reactor at a low organics-to-total nitrogen ratio in wastewater. *Folia Microbiol* 56:201–208
- Dennis KL, Wang Y, Blatner NR, Wang S, Saadalla A, Trudeau E, Roers A, Weaver CT, Lee JJ, Gilbert JA, Chang EB, Khazaie K (2013) Adenomatous polyps are driven by microbe-instigated focal inflammation and are controlled by IL-10-producing T cells. *Cancer Res* 73:5905–5913

- Ford DL, Kachtick JW (1980) Comprehensive analysis of nitrification of chemical processing wastewaters. *J Water Pollut Control Fed* 52:2726–2746
- Ganigué R, Volcke EIP, Puig S, Balaguer MD, Colprim J (2012) Impact of influent characteristics on a partial nitritation SBR treating high nitrogen loaded wastewater. *Bioresour Technol* 111:62–69
- Grady CPL, Daigger GT, Love NG, Filipe CDM (2011) *Biological wastewater treatment*, 3rd ed. CRC Press, London, pp. 99–102
- Greeneweg J, Sellner B, Tappe W (1994) Ammonia oxidation in nitrosomonas at NH_3 concentrations near km: effects of pH and temperature. *Water Res* 28:2561–2566
- Isanta E, Reino C, Carrera J, Perez J (2015) Stable partial nitritation for low-strength wastewater at low temperature in an aerobic granular reactor. *Water Res* 80:149–158
- Jemaat Z, Suarez-Ojeda ME, Perez J, Carrera J (2014) Partial nitritation and o-cresol removal with aerobic granular biomass in a continuous airlift reactor. *Water Res* 48:354–362
- Kim DJ, Seo DW, Lee SH, Shipin O (2012) Free nitrous acid selectively inhibits and eliminates nitrite oxidizers from nitrifying sequencing batch reactor. *Bioprocess Biosyst Eng* 35:441–448
- Kishida N, Saeki G, Tsuneda S, Sudo R (2012) Rapid start-up of a nitrifying reactor using aerobic granular sludge as seed sludge. *Water Sci Technol* 65:581–588
- Lackner S, Gilbert EM, Vlaeminck SE, Joss A, Horn H, van Loosdrecht MCM (2014) Full-scale partial nitritation/anammox experiences—an application survey. *Water Res* 55:292–303
- Li AJ, Yang SF, Li XY, Gu JD (2008) Microbial population dynamics during aerobic sludge granulation at different organic loading rates. *Water Res* 42:3552–3560
- Liang YH, Li D, Zeng HP, Zhang CD, Zhang J (2015) Rapid start-up and microbial characteristics of partial nitrification granular sludge treating domestic sewage at room temperature. *Bioresour Technol* 196:741–745
- Liu YQ, Wu WW, Tay JH, Wang JL (2008) Formation and long-term stability of nitrifying granules in a sequencing batch reactor. *Bioresour Technol* 99:3919–3922
- Ma B, Bao P, Wei Y, Zhu GB, Yuan ZG, Peng YZ (2015) Suppressing nitrite-oxidizing bacteria growth to achieve nitrogen removal from domestic wastewater via anammox using intermittent aeration with low dissolved oxygen. *Sci Rep* 5:13048–13057
- Ma B, Wang SY, Cao SB, Miao YY, Jia FX, Du R, Peng YZ (2016) Biological nitrogen removal from sewage via anammox: recent advances. *Bioresour Technol* 200:981–990
- Matsumoto S, Ishikawa D, Saeki G, Aoi Y, Tsuneda S (2010a) Microbial population dynamics and community structure during the formation of nitrifying granules to treat ammonia-rich inorganic wastewater. *Microbes Environ* 25:164–170
- Matsumoto S, Katoku M, Saeki G, Terada A, Aoi Y, Tsuneda S, Picioreanu C, van Loosdrecht MCM (2010b) Microbial community structure in autotrophic nitrifying granules characterized by experimental and simulation analyses. *Environ Microbiol* 12:192–206
- Mobarry BK, Wagner M, Urbain V, Rittmann BE, Stahl DA (1997) Phylogenetic probes for analyzing abundance and spatial organization of nitrifying bacteria. *Appl Environ Microbiol* 63:815–815
- Mosquera-Corral A, González F, Campos JL, Méndez R (2005) Partial nitrification in a SHARON reactor in the presence of salts and organic carbon compounds. *Process Biochem* 40:3109–3118
- Park S, Bae W, Rittmann BE (2010) Operational boundaries for nitrite accumulation in nitrification based on minimum/maximum substrate concentrations that include effects of oxygen limitation, pH, and free ammonia and free nitrous acid inhibition. *Environ Sci Technol* 44:335–342
- Perez J, Lotti T, Kleerebezem R, Picioreanu C, van Loosdrecht MC (2014) Outcompeting nitrite-oxidizing bacteria in single-stage nitrogen removal in sewage treatment plants: a model-based study. *Water Res* 66:208–218
- Rathnayake RM, Oshiki M, Ishii S, Segawa T, Satoh H, Okabe S (2015) Effects of dissolved oxygen and pH on nitrous oxide production rates in autotrophic partial nitrification granules. *Bioresour Technol* 197:15–22
- Shi XY, Sheng GP, Li XY, Yu HQ (2010) Operation of a sequencing batch reactor for cultivating autotrophic nitrifying granules. *Bioresour Technol* 101:2960–2964
- Show KY, Lee DJ, Tay JH (2012) Aerobic granulation: advances and challenges. *Appl Biochem Biotechnol* 167:1622–1640
- Sinha B, Annachatre AP (2006) Partial nitrification—operational parameters and microorganisms involved. *Rev Environ Sci Bio* 6:285–313
- Van H, Stijin WH, Vandeweyer HJP, Meesschaert BD, Vanrolleghem PA, Dejans P, Dumoulin A (2010) Engineering aspects and practical application of autotrophic nitrogen removal from nitrogen rich streams. *Chem Eng J* 162:1–20
- Vázquez-Padín JR, Figueroa M, Campos JL, Mosquera-Corral A, Méndez R (2010) Nitrifying granular systems: a suitable technology to obtain stable partial nitrification at room temperature. *Sep Purif Technol* 74:178–186
- Wan CL, Sun SP, Lee DJ, Liu X, Wang L, Yang X, Pan XL (2013) Partial nitrification using aerobic granules in continuous-flow reactor: rapid startup. *Bioresour Technol* 142:517–522
- Wan CL, Zhang QL, Lee DJ, Wang YY, Li JN (2014) Long-term storage of aerobic granules in liquid media: viable but non-culturable status. *Bioresour Technol* 166:464–470
- Wei D, Xue XD, Yan L, Sun M, Zhang G, Shi L, Du B (2014) Effect of influent ammonium concentration on the shift of full nitritation to partial nitrification in a sequencing batch reactor at ambient temperature. *Chem Eng J* 235:19–26
- Wu L, Peng CY, Peng YZ, Li LY, Wang SY, Ma Y (2012) Effect of wastewater COD/N ratio on aerobic nitrifying sludge granulation and microbial population shift. *J Environ Sci* 24:234–241
- Wu CY, Peng YZ, Wang SY, Ma Y (2010) Enhanced biological phosphorus removal by granular sludge: from macro- to micro-scale. *Water Res* 44:807–814
- Wu DL, Shen YH, Ding AQ, Mahmood Q, Liu S, Tu QP (2013) Effects of nanoscale zero-valent iron particles on biological nitrogen and phosphorus removal and microorganisms in activated sludge. *J Hazard Mater* 262:649–655
- Zhou Y, Oehmen A, Lim M, Vadivelu V, Ng WJ (2011) The role of nitrite and free nitrous acid (FNA) in wastewater treatment plants. *Water Res* 45:4672–4682